Tangential velocity profiles of granular material within horizontal rotating cylinders modelled using the DEM

J. R. Third · D. M. Scott · S. A. Scott · C. R. Müller

Abstract Flow regimes of granular materials in horizontal rotating cylinders are industrially important since they have a strong influence on the rates of heat and mass transfer within these systems. The tangential velocity profile, which describes how the average particle velocity in the direction parallel to the surface of the bed varies along a radius perpendicular to the surface of the bed, has been examined for many experimental and simulated systems. This paper is concerned with tangential velocity profiles within rotating cylinders simulated using the discrete element method. For high fill levels good agreement is found between the simulated velocity profiles and the equation proposed by Nakagawa et al. (Exp Fluids 16:54–60, 1993) based on magnetic resonance measurements. At lower fill levels slip is observed between the cylinder wall and the particles in contact with it and also between the outer layer of particles and the bulk of the bed. It is demonstrated that this slip occurs when the particles in contact with the wall are able to rotate and that it may be prevented either by using non-spherical particles or by attaching "lifters" to the cylinder wall.

J. R. Third (✉) · C. R. Müller
Department of Mechanical and Process Engineering,
Institute of Energy Technology, ETH Zürich, Leonhardstraße 27,
8092 Zürich, Switzerland
e-mail: jthird@ethz.ch

D. M. Scott
Department of Chemical Engineering and Biotechnology,
University of Cambridge, Pembroke Street, Cambridge, CB2 3RA,
UK

S. A. Scott
Department of Engineering, University of Cambridge, Trumpington
Street, Cambridge, CB2 1PZ, UK

List of Symbols

d_b	Diameter of attached particle for non-spherical particles, m
d_p	Nominal particle diameter, m
dt	Timestep, s
D	Diameter of cylinder, m
f	Cylinder fill level
F_n	Normal force between colliding particles, N
F_t	Tangential force between colliding particles, N
Fr	Froude number
g	Acceleration due to gravity, m/s^2
k_n	Normal spring stiffness, N/m
$k_{n,ij}$	Effective normal spring stiffness for a collision between particles i and j, N/m
k_t	Tangential spring stiffness, N/m
$k_{t,ij}$	Effective tangential spring stiffness for a collision between particles i and j, N/m
L	Length of cylinder, m
m	Particle mass, kg
m_{ij}	Effective mass in collision between particles i and j, kg
r	Radial coordinate, m
r_0	Radial coordinate of active/passive boundary, m
r_s	Radial coordinate of free surface, m
t_{col}	Duration of a collision, s
v_n	Relative velocity in normal direction, m/s
v_t	Relative velocity in tangential direction, m/s
V_m	Fitting parameter for (1), m/s
δ_n	Particle overlap, m
δ_t	Tangential displacement, m
ϵ	Half angle of the circular segment occupied by solids, deg
η_n	Damping factor in normal direction
η_t	Damping factor in tangential direction

μ_p	Inter-Particle coefficient of friction
μ_w^*	Wall-Particle coefficient of friction
μ_w^*	Critical wall-particle coefficient of friction
ρ	Particle density, kg/m^3
θ	Dynamic angle of repose, deg
ω	Cylinder rotation speed, rad/s
Ω	Cylinder rotation speed, rpm
$\hat{\Omega}$	Fitting parameter for (1), rad/s

1 Introduction

Rotary cylinders or kilns are widely used in industry for processes such as mixing, drying, coating and performing chemical reactions. Granular motion within these cylinders is also an area of significant research interest due to the rich array of phenomena exhibited [1–3]. Depending on the system conditions, several different flow regimes have been identified within rotating cylinders including: sliding, surging, avalanching, rolling, cascading, cataracting and centrifuging [4,5]. Industrial rotating cylinders are usually operated in the rolling or avalanching modes. Particle motion within the rolling regime is widely believed to comprise two regions: a passive region, in which the particles undergo rigid body rotation, and an active or flowing region, in which the particles flow down the free surface. This is shown schematically in Fig. 1.

This paper is concerned with rotating cylinders operating in the rolling regime and examines an aspect of particle motion within these systems that has received considerable academic attention: the "tangential velocity profile" (TVP). The TVP describes how the average particle velocity in the direction parallel to the surface of the bed varies along a
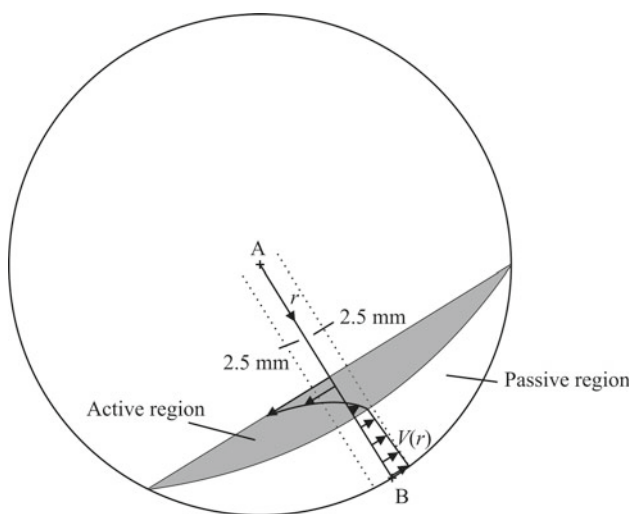
Fig. 1 Schematic showing the active and passive regions for a rotating cylinder operating in the rolling regime. The arrows show the tangential velocity profile at radius r

radius perpendicular to the surface of the bed (marked A–B in Fig. 1).

Nakagawa et al. [6] and Nakagawa et al. [7] have studied the flow of 1.5 mm mustard seeds within a cylinder of diameter 70 mm using magnetic resonance imaging. The fill level of the system was 50%. They found that particle motion within the passive region could be well described by rigid body rotation about the centre of the cylinder. Near the surface of the bed they found a region of constant shear and a non-zero velocity gradient at the free surface. Nakagawa et al. [7] observed that, at low speeds, the tangential velocity profile can be fitted by the expression:

$$V(r) = \begin{cases} V_m\left(1 - \dfrac{r}{r_0}\right)^2 - \hat{\Omega}r, & 0 \le r \le r_0 \\ -\hat{\Omega}r, & r_0 \le r \le \dfrac{D}{2} \end{cases} \quad (1)$$

where r is the radial distance from the centre of the cylinder, r_0 is the location of the interface between the flowing and passive regions, D is the cylinder diameter, $\hat{\Omega}$ is the angular velocity of the rigid body rotation and V_m is a parameter. V_m is the velocity at the free surface for the case of a fill level of 50% but has no physical meaning for lower fill levels. Note that, due to the possibility of slip between the cylinder wall and the bed, $\hat{\Omega}$ may be different to the angular velocity of the drum. For higher rotation rates, Nakagawa et al. [7] reported that the velocity near the surface of the bed was lower than predicted by the quadratic form given in (1). One explanation for this behaviour is that at higher speeds particles have more momentum perpendicular to the free surface and are therefore more likely to "unweight", such that their mass is not supported by contacts with particles below them, than when the bed is rotated more slowly. This theory is supported by experiments performed by Santratello et al. [8] who used a "paddle" to reduce the azimuthal velocity of particles approaching the free surface. The presence of this paddle was found to improve the fit between the experimental data and (1).

Parker et al. [9] and Ding et al. [10] have used positron emission particle tracking (PEPT) to investigate the tangential velocity profiles of beds composed of spherical glass beads. The systems studied by Parker et al. [9] are summarised in Table 1. In contrast to Nakagawa et al. [7], both Parker et al. [9] and Ding et al. [10] found the velocity gradient at the free surface to be zero for all rotation speeds. A second interesting feature reported by Parker et al. [9] is that, with the exception of 1.5 mm particles rotating at 13 rpm, the velocity of the cylinder wall was found to be higher than that of the particles in contact with it. Parker et al. [9] further investigated this slip by plotting the distributions of tangential velocities of particles close to the wall. For the systems which exhibit the most slip (large particles and high rotation speeds) these distributions were found to be bi-modal. This observation is consistent with the hypothesis that at the interface between

Table 1 Parameters for the experiments conducted by Parker et al. [9]

Cylinder diameter (mm)	Cylinder length (mm)	Particle diameter (mm)	Fill level (%)	Rotation speed (rpm)
136	750	1.5	32	13–54
144	350	3.0	33	18–63
100	650	3.0	36	10–65

the cylinder and the bed there are two layers of spheres rolling over one another: an inner layer travelling at the velocity of the bulk bed and an outer layer which is in contact with the cylinder and has a velocity between that of the bulk and the cylinder wall. Parker et al. [9] suggested that this slip is a consequence of using spherical particles and noted that it is probably not encountered in most systems of industrial interest.

Boateng and Barr [11] used an optic fibre probe to investigate beds consisting of either polyethylene spheres, limestone or rice grains. Over a range of rotation speeds and fill levels, Boateng and Barr [11] found that spherical particles gave an essentially uniform velocity gradient in the flowing layer. In some cases the data presented may be consistent with a velocity gradient that increases near the free surface. For the non-spherical materials linear velocity profiles were again found at low fill levels but parabolic velocity profiles, in which the velocity gradient approached zero at the free surface of the bed, were observed for higher fill levels. The deviation from a uniform velocity gradient was found to increase with fill level and cylinder rotation speed.

Tangential velocity profiles for systems simulated using the discrete element method (DEM) have been reported by Yamane et al. [12], Yang et al. [13] and Freireich et al. [14]. Yamane et al. [12] compared experiments and DEM simulations of the TVP of mustards seeds. At low speeds both experimental and simulated profiles were found to be well described by (1). Both Yang et al. [13] and Freireich et al. [14] simulated systems chosen to match the experiments of Parker et al. [9]: a drum diameter of 100 mm, particle size of 3 mm and a fill fraction of 35%. Within the active region, both authors found the velocity profiles from their DEM simulations agreed well with the experimental data of Parker et al. [9] except near the surface of the bed where the simulations were found to over-predict the velocity. Yang et al. [13] also found good agreement within the passive region but Freireich et al. [14] found the simulated velocity profile under-predicted the velocity in this region.

Based on the above, there are considerable discrepancies between both experiments and simulations and also between experiments conducted on different systems or using different techniques. As a result, the nature of the TVP and its dependence on the physical properties of the granular

material and the operating conditions of the cylinder remain unclear. In this work we attempt to elucidate some of these issues by making a detailed study of TVPs obtained for systems simulated using the DEM. We focus on the motion of particles close to the cylinder wall and examine the effect of fill level, friction coefficient and sphericity on the form of the TVP. Throughout this paper the cylinder diameter, cylinder rotation speed and the volume of the individual particles remain constant.

2 Simulation method

DEM for spheres is well documented in the literature [15] and will not be described here except to detail the particular force laws used in this work.

In the normal direction a damped linear spring is employed and attractive forces between particles are prevented such that the force in the normal direction, F_n, for a collision between particles i and j is given by:

$$F_n = \max\left(0, k_{n_{ij}}\delta_n - 2\eta_n\sqrt{\frac{m_{ij}}{k_{n_{ij}}}}v_n\right) \quad (2)$$

Here η_n is the damping factor in the normal direction, δ_n is the particle overlap and v_n is the relative velocity in the normal direction. m_{ij} is the effective mass defined as $1/m_{ij} = 1/m_i + 1/m_j$. $k_{n_{ij}}$ is the normal stiffness given by $1/k_{n_{ij}} = 1/k_{n_i} + 1/k_{n_j}$ where k_{n_i} is the normal stiffness of particle i. For the work presented here all particles have the same stiffness so $k_{n_{ij}} = k_{n_i}/2$. In the tangential direction static friction is modelled as a damped linear spring and the magnitude of the tangential force is limited by Coulomb's law such that

$$F_t = \min\left(\mu k_{n_{ij}}\delta_n, k_{t_{ij}}\delta_t - 2\eta_t\sqrt{\frac{m_{ij}}{k_{t_{ij}}}}v_t\right) \quad (3)$$

Here μ is the coefficient of friction, η_t is the damping factor in the tangential direction and v_t is the relative velocity of the two surfaces in contact. The tangential displacement, δ_t, is defined as $\int v_t dt$ and the tangential stiffness $k_{t_{ij}}$ is calculated in the same way as the normal stiffness. Table 2 shows the parameter values of the base case used in this work. The particle stiffness used in this work has been chosen to be lower than that of most real materials to allow the simulations to be completed within a manageable timescale. Freireich et al. [14] conducted an extensive study into the effect of contact properties on particle motion within rotating cylinders and found that flow level behaviour was "completely unaffected" by the choice of particle stiffness or coefficient of restitution. Consequently, the results presented here are not expected to depend strongly on the values chosen for the particle stiffnesses or the damping factors. The fill level of the base case

Table 2 Base case simulation parameters

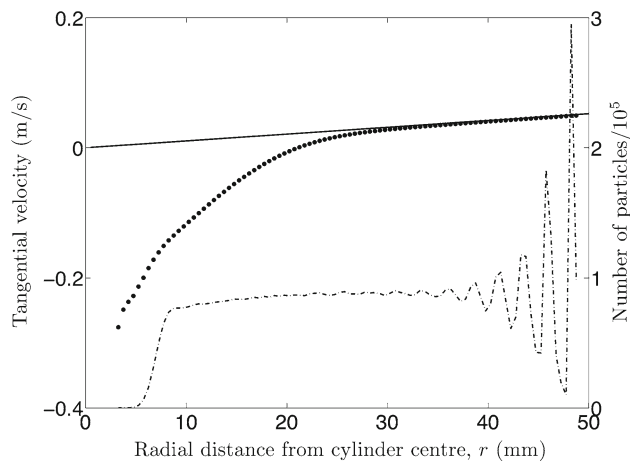| Name	Symbol	Value
Nominal particle diameter	d_p	3 mm
Particle density	ρ	2,500 kg/m^3
Normal spring stiffness	k_n	2,000 N/m
Tangential spring stiffness	k_t	1,000 N/m
Normal damping factor	η_n	0.22
Tangential damping factor	η_t	0.2
Particle coefficient of friction	μ_p	0.7
Acceleration due to gravity	g	9.81 m/s^2
Cylinder diameter	D	100 mm
Cylinder length	L	152 mm
Cylinder rotation speed	Ω	10 rpm
Number of particles	N	19,380

Fig. 2 Non-spherical particle composed of spheres with diameters d_p and d_b, where $d_b = d_p/2$

3 Calculating the tangential velocity profile

The tangential velocity profiles presented in this work have been calculated based on particles that lie within 2.5 mm of the plane containing the line A–B. Figure 1 shows a schematic of the particles in a cross-section that would contribute to the calculation of the tangential velocity profile. Authors including Boateng and Barr [11] and Yamane et al. [12] have shown that close to the cylinder end caps the transverse motion of the particles is different to that in the bulk of the bed. To eliminate the effect of the end caps, the calculation of the tangential velocity profiles is further restricted to particles in a 100 mm axial band at the centre of the cylinder. The tangential velocity profile is calculated by dividing the radius of the bed into slices parallel to the free surface and calculating the average particle velocity in the direction parallel to the free surface of the bed for each of these slices. In this work the radius of the cylinder is divided into 0.5 mm slices and, for the purpose of calculating the tangential velocity, the angle between the surface of the bed and the horizontal is assumed to be the time-averaged angle of repose.

4 Results and discussion

Figure 3 shows the tangential velocity profile for the system described in Table 2. Lines corresponding to rigid body rotation of Ω, the rotation speed of the cylinder, about the cylinder axis and the number of particles which contribute to the average velocity at each value of r are also displayed. It can be seen that the tangential velocity profile approaches rigid body rotation close to the cylinder wall but remains slightly below the line, indicating that there is a small amount of slip between the cylinder wall and the bed. At large r the number of particles averaged to obtain the tangential velocity oscillates with an amplitude that increases with r. This oscillation arises because the particles close to the cylinder wall are arranged in discrete layers: there are a large number

system, defined as the fraction of the cylinder occupied by particles and voids between particles, is approximately 42%. A particle size distribution given by

$$p(d) = \frac{d_{\min} d_{\max}}{d_{\max} - d_{\min}} \frac{1}{d^2}, \quad d_{\min} \le d \le d_{\max} \tag{4}$$

is used for all simulations [16]. Here $p(d)$ is the probability that a particle has a diameter of d. The bounds on this distribution, $d_{\min}$ and $d_{\max}$, are 95 and 105% of the nominal particle size. The cylinder in which the particles are rotated is modelled as a smooth, but frictional, cylinder with flat, frictionless end caps. Other than the friction coefficient of the end caps, the physical properties of the cylinder and end caps are identical to those of the particles.

An area that is becoming increasingly important in DEM is the effect of non-spherical particles. One simple method for creating non-spherical particles is to create particles by gluing spheres together. This has the advantage that contact detection is unchanged compared to the spherical particle case. The non-spherical particles considered here consist of a large sphere of diameter d_p and a sphere of diameter d_b arranged so that they touch but do not overlap, Fig. 2. For non-spherical particles the equations of motion are applied to the particle as a whole rather than to the individual component spheres. Consequently, no forces are modelled between the component spheres that make up a non-spherical particle.

For all the simulations presented here, the equations of motion of the particles are integrated using a third order Adams-Bashforth scheme. The timestep of the numerical scheme, dt, is chosen such that it satisfies the equation $dt \le t_{col}/30$, where t_{col} is the duration of a collision.

Fig. 3 *Points* tangential velocity profile for 19,380, 3 mm particles in a cylinder of diameter 100 mm and length 152 mm. The cylinder is rotated at 10 rpm. *Solid line* rigid body rotation at cylinder rotation speed. *Dashed line* number of particles contributing to the average velocity

Fig. 4 *Points* tangential velocity profile for 19,380, 3 mm particles in a cylinder of diameter 100 mm and length 152 mm. The cylinder is rotated at 10 rpm. *Lines* (1) with $\hat{\Omega} = 10$ rpm, $r_0 = 29$ mm and $V_m = 0.302$ m/s

of particles for r corresponding to the centre of a layer while between layers there are very few particles.

Figure 3 shows that the number of particles that contribute to the TVP decreases rapidly for $r < 7.5$ mm, indicating that the free surface of the bed is located near this radius. In this work the radial coordinate of the free surface will be denoted r_s. For the system shown in Fig. 3 $r_s \approx 7.5$ mm. It can be seen that there is a corresponding increase in the gradient of the tangential velocity profile at this point.

Figure 4 shows the result of fitting the velocity profile proposed by Nakagawa et al. [7], (1), to the velocity profile shown in Fig. 3 for $r > 7.5$ mm. The fit assumes that the rotation speed of the rigid body rotation, $\hat{\Omega}$, is equal to the cylinder rotation speed of 10 rpm. To fit (1) to the data, r_0 was adjusted manually and V_m was then calculated using a least-squares fit for data in the range 7.5 mm $\leq r \leq r_0$. The velocity profile of Nakagawa et al. [7] fits the data well in the active region for 7.5 mm $< r < 23$ mm and makes the change in gradient of the simulation data at r_s clearly visible. Equation (1) was derived assuming constant voidage within the bed but for $r < 7.5$ mm the voidage decreases rapidly, as shown by the number of particles used in the calculation of the average velocity, and (1) is not expected to apply.

Experimental evidence suggests that the form of the TVP depends on both the operating conditions and the nature of the granular material. For $r > r_s$ the velocity profile presented in Fig. 3 appears to be consistent with published works that report a uniform velocity gradient close to the free surface of the bed. However, for $r < r_s$ the gradient of the velocity profile shown here increases. With the possible exception of the profiles reported for polyethylene spheres [11], this result appears contrary to published TVPs. One possible reason for
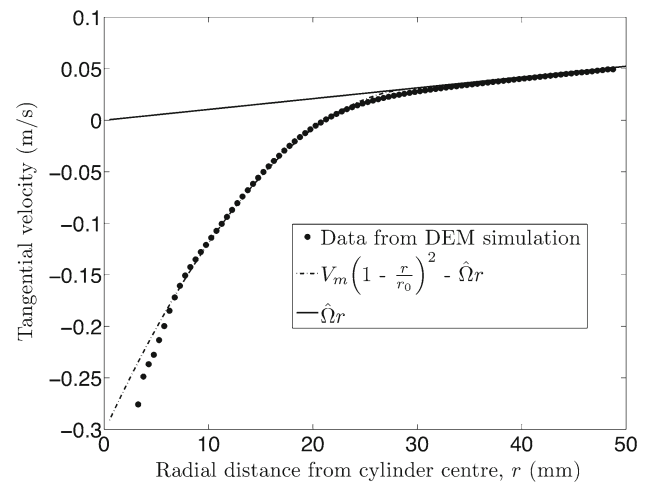
this discrepancy might be the trend for DEM simulations to over-predict the velocity of particles near the surface [13,14]. Alternatively, the velocity profile shown here may cover a wider range of r than those previously reported. Neither the location of the free surface nor the number of particles that contribute to the average velocity at each value of r are normally reported, with the result that it is not clear whether published velocity profiles are restricted to $r > r_s$.

If the number of particles is reduced to 11,220, equating to a fill level of approximately 25%, the behaviour is dramatically different. Figure 5 shows TVPs for this fill level with a range of values of friction coefficient. The indicated values of μ are applied for both particle-particle and particle-cylinder interactions. For $\mu = 1.0$ the velocity profile is similar to that shown in Fig. 3. However the slip observed by Parker et al. [9] is present: the outermost particles have a tangential velocity lower than the wall speed and there is a kink in the velocity profile which suggests that the outermost particles are rotating slightly faster than the rest of the bed. As μ is decreased this slip becomes more pronounced: the velocity of the outermost particles decreases and the speed difference between the outermost particles and the second layer of particles increases. For $\mu = 0.5$ and $\mu = 0.3$ there is a central core of particles which are almost stationary. The region outside of this core consists of a single layer of particles which are lifted by the cylinder wall and flow down the free surface.

Mellmann [5] proposed that the transition between the slipping and cascading regimes may be described by a critical value of the cylinder friction coefficient:

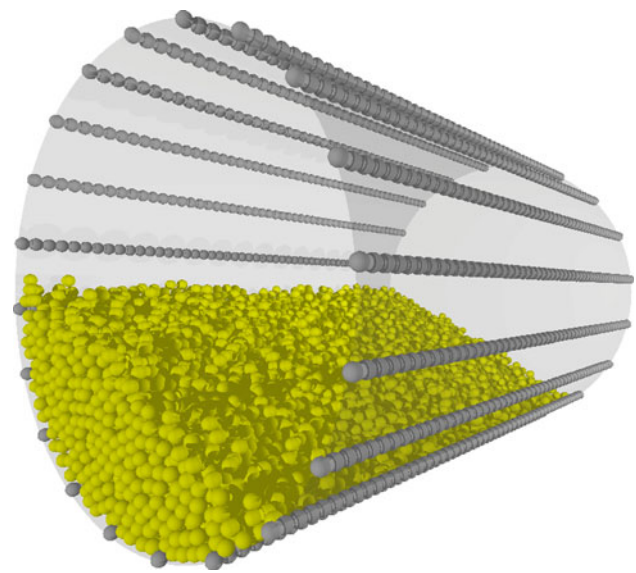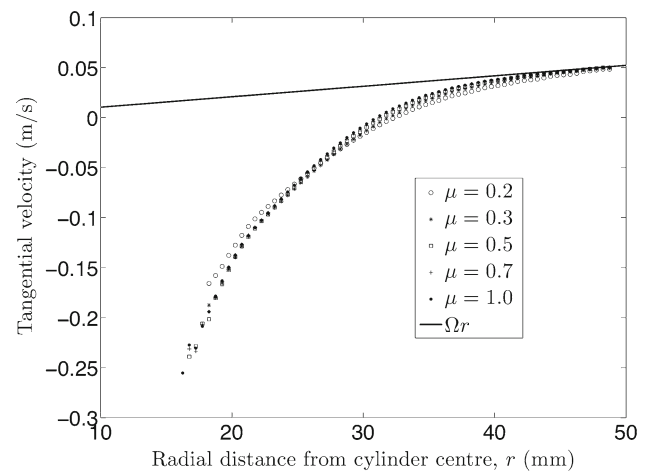$$\mu_w^* = \frac{2\sin^3 \epsilon \sin \theta}{3\pi f (1 + Fr)} \tag{5}$$
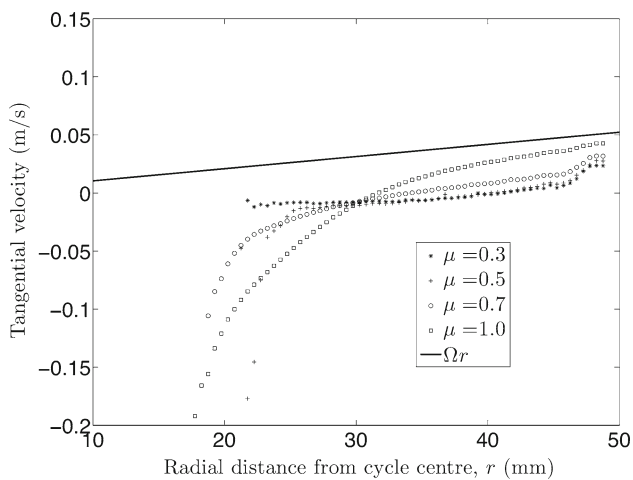
Fig. 5 Tangential velocity profiles for a range of coefficients of friction for $f = 26\%$. The particles are 3 mm spheres and the cylinder has a diameter of 100 mm, a length of 152 mm and is rotated at 10 rpm

where ϵ is the half angle of the circular segment occupied by solids, θ is the dynamic angle of repose, f is the cylinder fill fraction and Fr is the Froude number defined as $\omega^2 D/2g$. Here ω is the rotational speed of the cylinder in rad/s. For the $\mu = 0.7$ case shown in Fig. 5 ($\epsilon = 67°$, $\theta = 25°$), (5) gives $\mu_w^* = 0.27$. Therefore, based on Mellmann's criterion, the systems shown in Fig. 5 should be expected to operate within the rolling regime. It should be noted that the bed regime shown in Fig. 3 is distinct from both the slipping and surging regimes described by Mellmann [5]. In those regimes there is no relative motion within the bed and slip occurs between the bed and the cylinder wall. In the regime reported here slip occurs between both the cylinder wall and the bed and between the outermost layer of particles and the bulk of the bed.

The slip demonstrated above may be prevented by attaching "lifters" to the cylinder wall, as used previously by Third et al. [17]. The lifters are created using lines of particles running along the length of the cylinder. The diameter of these lifter particles is the nominal diameter of the particles in the simulation and the lifters are spaced 5 particles diameters apart, centre to centre, around the cylinder circumference. The centres of the lifter particles are placed a distance $\frac{D}{2}$ from the axis of the cylinder so that only half of the lifter particle protrudes on the inside of the cylinder. Figure 6 shows an example of such a cylinder with lifters made of 3 mm particles. Creating lifters in this way is similar to many experimental setups where sandpaper or particles are glued onto the inner surface of the cylinder to prevent slip between the cylinder and the bed [10]. Figure 7 shows the tangential velocity profiles for 11,220, 3 mm particles in a cylinder with lifters. The system is identical to that used to generate the profiles shown in Fig. 5 except that lifters have been attached to the cylinder wall. The velocity profiles are similar for all values


Fig. 6 Horizontal drum of diameter 100 mm and length 152 mm with lifters made of 3 mm particles

Fig. 7 Tangential velocity profiles for a range of coefficients of friction for $f = 26\%$ with lifters. The particles are 3 mm spheres and the cylinder has a diameter of 100 mm, a length of 152 mm and is rotated at 10 rpm

of μ and take a form similar to that shown in Fig. 3. There is little or no slip at the cylinder wall.

The velocity profiles shown in Fig. 5 may be the result of a more exaggerated form of the slip observed experimentally by Parker et al. [9]. To investigate further the particle motion within this system we analyse the rotation of the particles about their centres of mass, which we term "spin". In this work only the component of particle spin about an axis that is parallel to the axis of the cylinder shall be considered. Figure 8 shows average particle spin as a function of radial position for systems simulated with and without lifters. For both systems the fill level is 25% and the coefficient of friction for both particle-wall and particle-particle contacts is
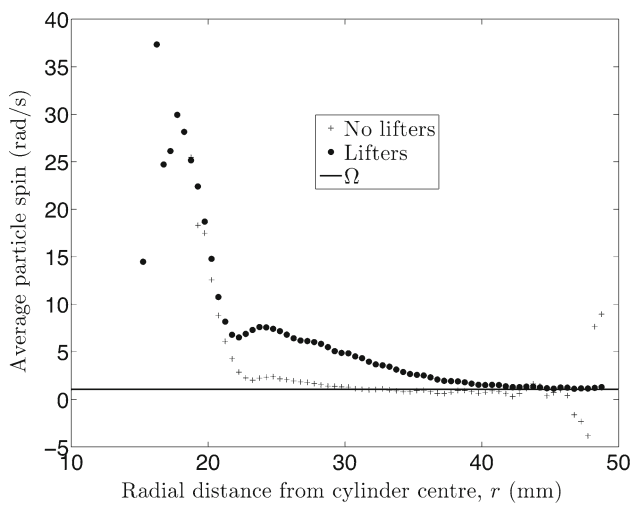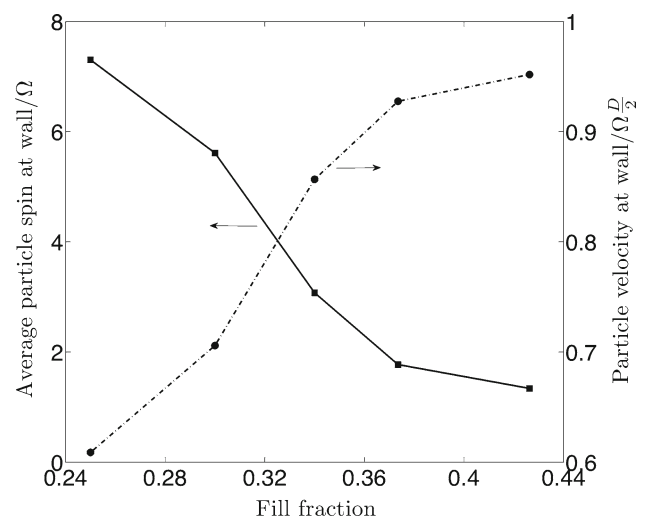
Fig. 8 Spin profiles for systems simulated with and without lifters for a fill level of 26%. The particles are 3 mm spheres and the cylinder has a diameter of 100 mm, a length of 152 mm and is rotated at 10 rpm
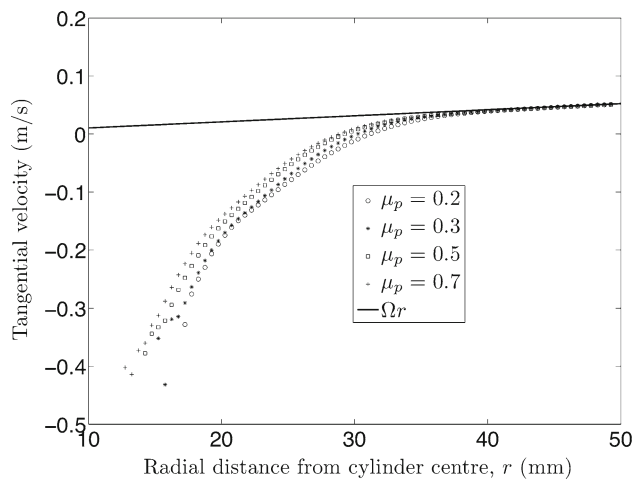

Fig. 9 Average dimensionless tangential velocities and spins for particles in contact with the cylinder wall shown as a function of fill fraction. The particles are 3 mm spheres and the cylinder has a diameter of 100 mm, a length of 152 mm and is rotated at 10 rpm

$\mu = 0.7$. A line corresponding to $\Omega = 10$ rpm ($\pi/3$ rad/s) is also shown. The presence of lifters has a dramatic effect on the spin profile within the bed. For the system with lifters the particles close to the wall have a spin that is slightly above Ω but, when lifters are not present, these particles rotate significantly faster. It should be noted that the negative spins shown in Fig. 8 occur at a radius that is between the discrete layers of particles and consequently only a few particles are rotating in this direction.

The data presented in Figs. 5 and 8 suggest that the behaviour of particles close to the cylinder wall may be used to characterise whether the bed is operating in the rolling regime or the slipping regime that has been described here. Figure 9 shows the average tangential velocity and spin of particles in contact with the wall for a range of fill fractions. Both the tangential velocity and spin have been made dimensionless by dividing by the cylinder wall speed. These data suggest a smooth transition between slipping and rolling as the fill level is increased. Note that for these data the centres of the outermost particles are located at $r \approx 48.5$ mm with the result that a bed operating in the rolling regime would have a dimensionless tangential velocity of 0.97 on Fig. 9.

Figure 10 shows the effect of lifters on the $f = 42\%$ case considered above. The simulation parameters for the two cases shown are identical other than the addition of the lifters. The tangential velocity profiles with and without lifters are similar and the dynamic angle of repose is 27.4° for both systems. These data suggest that lifters prevent slip at low fill levels but do not significantly affect the behaviour of systems with a higher fill level. It is therefore proposed here that lifters may represent a practical method for simulating granular motion within rotating cylinders with a low fill level using the DEM.
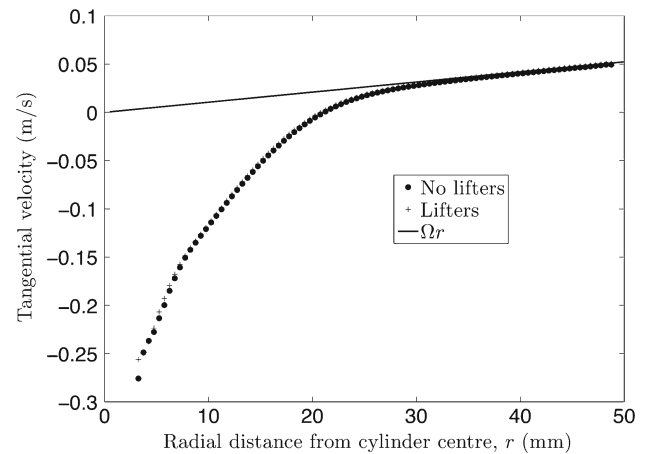
Fig. 10 Comparison of tangential velocity profiles with and without lifters for $f = 42\%$. The particles are 3 mm spheres, the cylinder has a diameter of 100 mm, a length of 152 mm and is rotated at 10 rpm

The data presented in Fig. 8 suggest that slip may be prevented by controlling the rotation of particles within the passive region. A second mechanism by which particle rotation may be inhibited is to simulate non-spherical particles. Figure 11 shows tangential velocity profiles for 11,220 non-spherical particles in a cylinder of diameter 100 mm and length 152 mm rotating at 10 rpm. The nominal value of d_p is 2.88 mm and $d_b = d_p/2$. Under these conditions the non-spherical particles have the same volume as the 3 mm spherical particles. A distribution of particle sizes is generated using (4). The fill level for this system is approximately 28% but, unlike spheres, the fill level for these particles depends noticeably on the particle-particle coefficient of friction, μ_p, as can be seen in Fig. 11. The material properties

Fig. 11 Tangential velocity profiles for 11,220 non-spherical particles with $d_b = 2.88$ mm and $d_b = d_p/2$. The cylinder has a diameter of 100 mm, a length of 152 mm and is rotated at 10 rpm. The fill level is approximately 28%
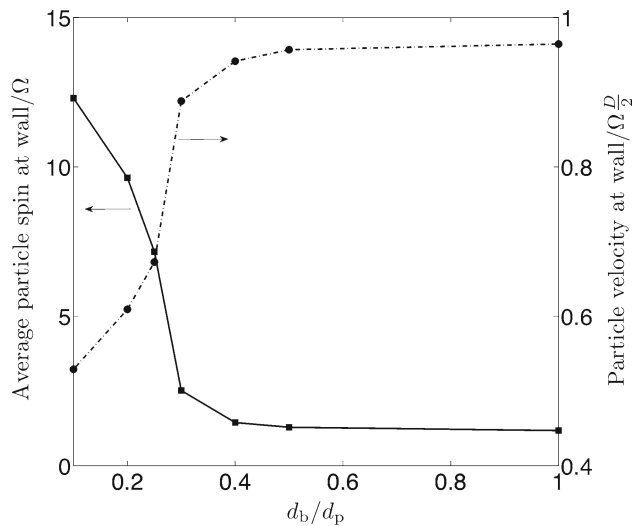
Fig. 12 Average dimensionless tangential velocities and spins for particles in contact with the cylinder wall shown as a function of d_b/d_p. The cylinder has a diameter of 100 mm, a length of 152 mm and is rotated at 10 rpm

of the non-spherical particles are the same as those given in Table 2 except for the coefficient of friction for particle-wall contacts, μ_w. For $\mu_w = 0.3$, the system described here operates in "slipping" mode, characterised by a rigid body that slides at the bed-wall interface, rather than the desired rolling mode. Consequently the simulations of non-spherical particles shown here use $\mu_w = 0.7$ rather than $\mu_w = \mu_p$ as was used for the spherical particles. This is again comparable with the experimental practice of roughening the cylinder wall the prevent slip. Furthermore, spheres with $\mu_w = \mu_p = 0.7$ show considerable slip (Fig. 5); the lack of slip for these non-spherical particles with $\mu_p = 0.7$ demonstrates that particle

shape is an important factor in preventing slip. The tangential velocity profiles in Fig. 11 show the same behaviour as those obtained for spherical particles when lifters are included: they are well described by (1) for $r > r_s$ and show an increase in gradient at $r = r_s$.

To investigate the effect of particle sphericity on the TVP, simulations have been performed for different values of the ratio d_b/d_p. These systems consist of 11,220 non-spherical particles and the value of d_p is adjusted so that particle volume is equal to the volume of a 3 mm sphere. Figure 12 shows the tangential velocities and spins of particles in contact with the cylinder wall for a range of values of d_b/d_p. These data suggest that the behaviour of this system depends strongly on the particle sphericity. For $d_b/d_p > 0.4$ there is little rotation at the wall and the bed operates in the rolling regime, whereas a significant particle spin is observed for $d_b/d_p < 0.3$.

5 Conclusions

Tangential velocity profiles for systems simulated using the DEM have been calculated. For a fill level of 42% the profile obtained is consistent with the quadratic form proposed by Nakagawa et al. [7]. At a fill level of 25% slip is observed between both the cylinder wall and the outer layer of particles and between the outer layer of particles and the bulk of the bed. This slipping regime, which is distinct from sliding or surging regimes identified by Mellmann [5], is thought to be a more pronounced form of the slip observed experimentally for spherical glass beads by Parker et al. [9].

It has been demonstrated that slip may be prevented at low fill levels by preventing relative rotation within the passive region. This may be achieved either by attaching "lifters" to the cylinder wall or, when a high coefficient of friction is used for particle-wall contacts, by changing the particle shape. It is proposed that both of these techniques are practical solutions to modelling rotating cylinders with low fill levels using the DEM. Further work is required to understand why slip occurs at low fill levels but is not present at high fill levels.

References

1. Dury, C.M., Ristow, G.H.: Axial particle difusion in rotating cylinders. Granul. Matter **1**, 151–161 (1999)
2. Rapaport, D.C.: Simulation studies of axial segregation in a rotating cylinder. Phys. Rev. E **65**, 061306 (2002)
3. Chou, H.-T., Lee, C.-F.: Cross-sectional and axial flow characteristics of dry granular material in rotating drums. Granul. Matter **11**, 13–32 (2009)

4. Henein, H., Brimacombe, J.K., Watkinson, A.P.: Experimental studies of transverse bed motion in rotary kilns. Metall. Trans. B. **14B**, 191–205 (1983)

5. Mellmann, J.: The transverse motion of solids in rotating cylinders—forms of motion and transition behavior. Powder Technol. **118**, 251–270 (2001)

6. Nakagawa, M., Altobelli, S.A., Caprihan, A., Fukushima, E., Jeong, E.-K.: Non-invasive measurements of granular flow by magnetic resonance imaging. Exp. Fluids **16**, 54–60 (1993)

7. Nakagawa, M., Altobelli, S.A., Caprihan, A., Fukushima, E.: NMR measurement and approximate derivation of the velocity depth-profile of granular flow in a rotating, partially filled, horizontal cylinder. In: Behringer, R.P., Jenkins, J.T. (eds.) Powders and Grains 97., pp. 447–450. Balkema, Rotterdam (1997)

8. Sanfratello, L., Caprihan, A., Fukushima, E.: Velocity depth profile of granular matter in a horizontal rotating drum. Granul. Matter **9**, 1–6 (2007)

9. Parker, D.J., Djkstra, A.E., Martin, T.W., Seville, J.P.K.: Positron emission particle tracking studies of spherical particle motion in rotating drums. Chem. Eng. Sci. **52**, 2011–2022 (1997)

10. Ding, Y.L., Seville, J.P.K., Forster, R., Parker, D.J.: Solids motion in rolling mode rotating drums operated at low to medium rotational speeds. Chem. Eng. Sci. **64**, 3407–3416 (2001)

11. Boateng, A.A., Barr, P.V.: Granular flow behaviour in the transverse plane of a partially filled rotating cylinder. J. Fluid Mech. **330**, 233–249 (1997)

12. Yamane, K., Nakagawa, M., Altobelli, S.A., Tanaka, T., Tsuji, Y.: Steady particulate flow in a horizontal rotating cylinder. Phys. Fluids **10**, 1419–1427 (1998)

13. Yang, R.Y., Zou, R.P., Yu, A.B.: Microdynamic analysis of particle flow in a horizontal rotating drum. Powder Technol. **130**, 138–146 (2003)

14. Freireich, B., Litster, J., Wassgren, C.: Using the discrete element method to predict collision-scale behavior: a sensitivity analysis. Chem. Eng. Sci. **64**, 3407–3416 (2009)

15. Cundall, P.A., Strack, O.D.L.: A discrete numerical model for granular assemblies. Geotechnique **29**, 47–65 (1978)

16. Pöschel, T., Schwager, T.: Computational Granular Dynamics: Models and Algorithms. Springer, Berlin (2005)

17. Third, J.R., Scott, D.M., Scott, S.A.: Axial dispersion of granular material in horizontal rotating cylinders. Powder Technol (2009). doi:10.1016/j.powtec.2010.06.017